Flavonoids with Herbicidal, Fungicidal, Insecticidal, Molluscicidal, and Larvicidal Potential: SAR and Molecular Dynamics Insights

A. Immaculate, A. Kalpana*

PG & Research Department of Chemistry, Sri Sarada College for Women, Salem, Tamil Nadu 636 016, India.

kalpanaanbarasu@gmail.com

Keywords: *Flavonoid derivatives, Eco-friendly agrochemicals, Computational agrochemistry, SAR analysis, Simulation studies*

This study presents a computational evaluation of 140 flavonoid derivatives (chrysin, hesperetin, apigenin, naringenin, and quercetin) for agrochemical potential. A three-tier screening approach was applied: physicochemical profiling confirmed compliance with Lipinski's Rule of Five and indicated strong molluscicidal and larvicidal potential; molecular docking revealed multi-target activity, with chrysin, naringenin, and hesperetin as dominant scaffolds, while apigenin-IIa showed consistent herbicidal activity; ADMET analysis identified several non-toxic, stable scaffolds. Key potential agrochemical candidates, including Chrysin Ia, Naringenin IIIa/b, Apigenin IIa, and Quercetin V, were prioritized. Sixteen active derivatives were selected for SAR studies, and molecular dynamics simulations confirmed stable binding interactions and favourable energetics.

Introduction

The growing demand for sustainable agricultural production has intensified the need for effective crop protection strategies against weeds, insects, fungi, molluscs, and other agricultural pests. Although some pesticides have played a pivotal role in enhancing crop productivity, their prolonged and indiscriminate use has resulted in environmental contamination, non-target toxicity, bioaccumulation and the rapid emergence of pesticide-resistant pest populations. These concerns have stimulated global efforts to identify environmentally benign and biologically effective alternatives that can support sustainable crop protection while minimizing ecological risks. Among the natural product classes explored for agrochemical development, flavonoids have emerged as promising candidates due to their abundance in plants and broad spectrum of biological activities. Flavonoids are a diverse group of polyphenolic secondary metabolites that contribute to plant defence against biotic and abiotic stresses, interspecies signalling, UV protection, and pigmentation [1-3]. Their inherent biodegradability, relatively low mammalian toxicity, and structural diversity make them attractive scaffolds for the development of next-generation agrochemicals. Numerous naturally occurring flavonoids, including quercetin, apigenin, kaempferol, and their glycosides, have demonstrated pesticidal activities against a wide range of agricultural pests and pathogens [1]. Several flavonoids exhibit insecticidal and antifeedant activities by disrupting feeding behaviour, growth, and

development of economically important insect pests. For example, quercetin and luteolin have been shown to interfere with aphid feeding behaviour, whereas apigenin and related compounds exhibit significant antifeedant effects against crop-damaging insects [1]. In addition, flavonoids possess herbicidal potential through allelopathic mechanisms that inhibit seed germination, root elongation, and seedling growth of competing plant species [4]. Their reported antifungal, larvicidal, and molluscicidal activities further highlight their potential as multifunctional agrochemical agents [5-7].

Despite these promising findings, the practical utilization of flavonoids as agrochemicals remains constrained by several challenges. Natural flavonoids often exhibit variable physicochemical properties, limited environmental persistence, and inconsistent biological efficacy. Previous studies have demonstrated that structural features strongly influence flavonoid stability, with highly hydroxylated compounds degrading more rapidly in soil than their methoxylated counterparts, underscoring the importance of structure-dependent behaviour in agrochemical performance [8]. More importantly, existing research has predominantly focused on naturally occurring flavonoids or individual pesticidal activities, providing only fragmented insights across different agricultural targets [1-8].

Synthetic derivatization of flavonoid scaffolds offers an effective strategy to overcome these limitations and enhance agrochemical performance. Structural modification can improve stability, bioavailability, target affinity, and environmental compatibility while expanding the chemical space available for agrochemical discovery. In particular, synthetic derivatives of chrysin, apigenin, naringenin, hesperetin, and quercetin have attracted growing interest because these scaffolds provide versatile platforms for introducing functional groups capable of modulating biological activity [1,9]. However, despite the increasing number of synthetic flavonoid derivatives reported in the literature, their agrochemical potential has not been systematically investigated across multiple pesticidal targets.

This knowledge gap is scientifically significant because modern crop protection increasingly requires agrochemicals capable of controlling multiple agricultural threats while reducing overall pesticide usage and mitigating resistance development. The identification of broad-spectrum agrochemical candidates that can act against different classes of pests, as well as target-selective compounds with enhanced specificity, represents a major challenge in contemporary agrochemical research. Furthermore, a comprehensive understanding of the structure–activity relationships governing the pesticidal behaviour of synthetic flavonoids remains largely unexplored. Such information is essential for the rational design of environmentally sustainable agrochemicals with improved efficacy and safety profiles.

Recent advances in computational agrochemical discovery provide powerful tools for addressing these challenges. Integrated in silico approaches combining physicochemical profiling, molecular docking, toxicity prediction,

environmental fate assessment, and ADMET analyses enable the rapid evaluation of large compound libraries while reducing experimental cost and resource requirements [10]. These approaches also facilitate the identification of key structural determinants responsible for biological activity and target selectivity, thereby accelerating potential candidate optimization and agrochemical development.

Therefore, the present study undertakes a comprehensive computational evaluation of literature-reported synthetic derivatives of chrysin, apigenin, naringenin, hesperetin, and quercetin [11-23]. Using a systematic three-tier screening framework, the study integrates physicochemical assessment, molecular docking, toxicity prediction, and environmental compatibility analyses to identify promising agrochemical candidates. Unlike previous studies that primarily focused on individual flavonoids or single pesticidal activities, this work aims to simultaneously investigate herbicidal, fungicidal, insecticidal, molluscicidal, and larvicidal potential, enabling the identification of both multi-target and target-selective flavonoid derivatives. In addition to discovering promising candidate, the study provides valuable structure–activity relationship insights into how specific synthetic modifications influence agrochemical performance. The findings are expected to contribute to the rational design of sustainable flavonoid-based agrochemicals and provide new molecular templates for the development of next-generation environmentally friendly crop protection agents.

Materials and methods

Literature-reported synthetic derivatives of chrysin (Ia: **1-13**), (Ib1 **14-16**), (Ib2 **17-20**), (Ib3 **21-23**), (Ic **24-26**), (Id **27-29**), (Ie **30**), apigenin (IIa **31-47**), (IIb **48-50**), naringenin (IIIa **51-69**), (IIIb **70-80**), (IIIc **81-92**), hesperetin (IVa1 **93-97**), (Iva2 **98-101**), (IVb1 **102-110**), (IVb2 **111-117**), (IVc1 **118-125**), (IVc2 **126-128**) and quercetin (V **129-140**) were selected for this study **(Figure 1)** [11-23]. The group number, compound number, IUPAC name, chemical structure and SMILE of the compounds and references are given in **Table S1**.

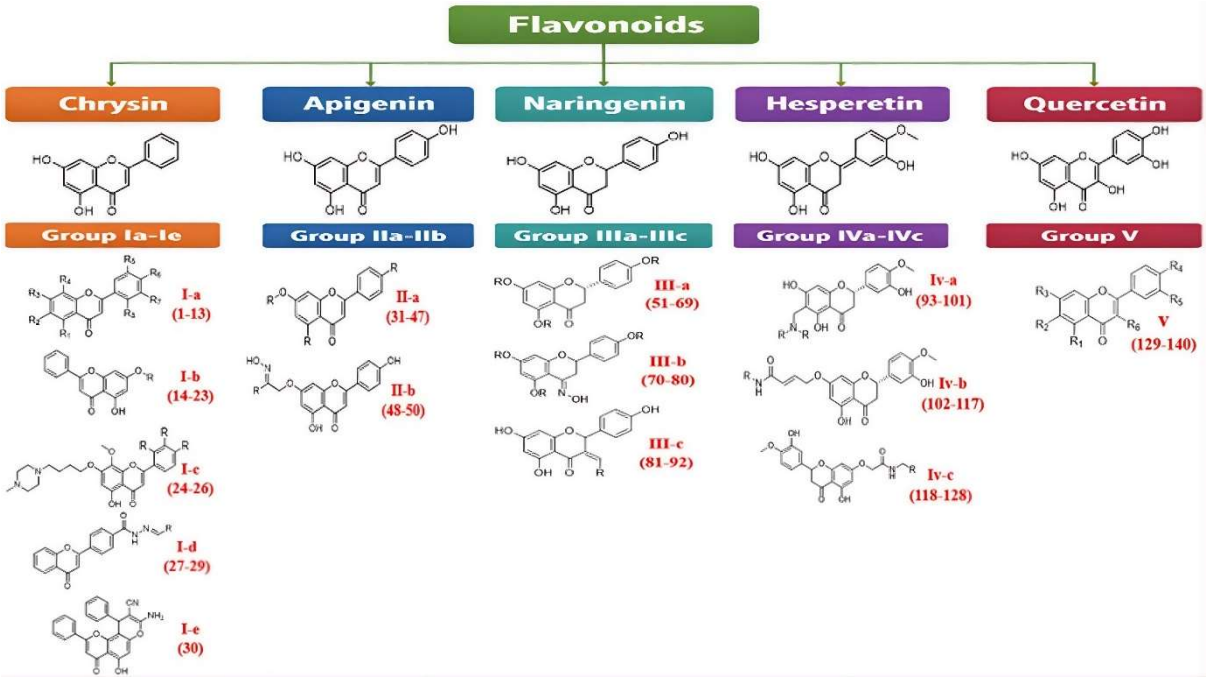

Figure 1. Flavonoids-Chrysin, -Apigenin, -Naringenin, -Hesperetin, and -Quercetin derivatives.

Molecular docking studies

The geometrical structures of flavonoid derivatives and reference pesticides were optimized using the Chem3D program with the MM2 force field method. The derivatives were docked against five critical protein targets. Pesticidal targets with associated activities and biological roles are presented in (**Table 1**). The crystal structures of proteins were obtained from the Protein Data Bank. Ligands, cofactors, and water molecules are removed from the protein to ensure accurate docking simulations. Docking was performed using Auto Dock Tools [24]. The energy grid was built within a cubic box and docking was performed based on Lamarckian genetic algorithm. Receptor grid was developed using Auto Dock Grid tool with grid dimensions of 80 Å × 80 Å × 80 Å with 1 Å spacing (UPO), of 80 Å × 80 Å × 80 Å with 1 Å spacing (GABA), 70 Å × 70 Å × 70 Å with 1 Å spacing (SDH), 90 Å × 74 Å × 80 Å with 1 Å spacing (AChE) of 40 Å × 40 Å × 40 Å with 1 Å spacing (JHBP). Docking was done in ten different orientations. The orientation with best binding energy was chosen and analysed using UCSF Chimera [25]. Biovia Discovery Studio [26] was employed for visualization and to examine the stabilizing interactions of the docked complexes.

Table 1. Pesticidal targets with associated activities and biological roles [27-31].

A*	B*	C*
Herbicidal	Unspecific Peroxygenase (UPO) (PDB: 7ZCL)	Catalyzes diverse oxidative reactions, including xenobiotic and plant metabolite degradation. Plays a role in herbicide detoxification.
Insecticidal	GABA (Gamma-aminobutyric acid) receptor (PDB: 5TIN)	A ligand-gated chloride channel crucial for inhibitory neurotransmission in insects.
Fungicidal	Succinate Dehydrogenase (SDH) (PDB: 2WQY)	Central enzyme of the TCA cycle and electron transport chain.
Molluscicidal	Acetylcholinesterase (AChE) (PDB: 1ACJ)	Hydrolyzes acetylcholine to terminate synaptic transmission.
Larvicidal	Juvenile Hormone Binding Protein (JHBP) (PDB: 2WID)	Transports and stabilizes juvenile hormone in insect hemolymph to regulate growth and development.

A*-Activity; B*-Target; C*-Significance.

ADMET Studies

ADMET properties of flavonoid derivatives and reference pesticides such as solubility, molecular weight, Lipophilicity, Total polar surface area, hydrogen bond Donar, hydrogen bond acceptor, rotatable bonds, gastrointestinal absorption, P-glycoprotein substrate, skin permeation, bioavailability are predicted by using Swiss ADME [32]. Safety profiles such as carcinogenicity, rat acute toxicity, skin sensitization, eye irritant, eye corrosive, herg, biodegradation, cytochrome inhibitors, plasma protein binding were forecast by using Deep pkCSM [33], and PreADMET [34]. Hepatotoxicity and central nervous system were foreseen using pkCSM [35] web tool. The Bioaccumulation Factor (BAF, L/kg wet weight) values were obtained from the ECOSAR web-based tool [36], which estimates the tendency of chemicals to accumulate in aquatic organisms based on their physicochemical properties and structural characteristics.

Molecular Dynamics Simulation

Molecular dynamics simulations of the top-ranked protein–ligand complexes were performed using GROMACS 2025.0 [37] with the CHARMM27 force field. Each complex was solvated in either a dodecahedral box (for Herbicidal and mosquitocidal targets) filled with TIP3P water molecules, ensuring a 1.0 nm buffer from the protein surface, followed by neutralization with 0.15 M NaCl. Energy minimization was achieved using the steepest descent method (10 ns/25 ns). Subsequently, equilibration was carried out under both NVT and NPT ensembles (10 ps each), applying a V-rescale thermostat at 300 K and pressure coupling at 1 atm. Production runs were executed for 10 ns/25 ns, employing the Particle Mesh Ewald method for long-range electrostatics and the LINCS algorithm to constrain covalent bonds. RMSD was calculated using backbone atoms and the trajectories were properly fitted and centered.

Results and discussion

In this study, a total of 140 flavonoid derivatives (**Figure 1**) were evaluated for their pesticide-likeness. Initially flavonoid derivatives were screened for their compliance with basic physicochemical requirements, ensuring

pesticide-likeness. Then the derivatives were docked against five critical protein targets (**Table 1**). Compounds showing binding affinity scores ≥ -7 kcal/mol were considered as potential candidates. Compounds passing the docking threshold were further analysed for pharmacokinetic behaviour and toxicity risk, to ensure safety and environmental compatibility. Finally, the top potential agrochemical candidate compounds were identified and their structure–activity relationships were discussed to establish flavonoid-based agrochemicals.

The principal physicochemical criteria, together with the number of compounds meeting each requirement, are summarized in **Table 2** and elaborated in **Tables S2-S6**. These selection parameters were derived from established guidelines, such as Lipinski's rule of five and Tice's rule, which are widely applied in the rational design and assessment of agrochemical candidates [20-25]. The selection thresholds were established based on molecular weight, lipophilicity, topological polar surface area, hydrogen bond donors, hydrogen bond acceptors, and rotatable bonds, which are known to influence membrane permeability, target-site accessibility, binding affinity, and overall bioactivity. Aligning the properties of flavonoid derivatives with these benchmarks provides insights into their potential efficacy and environmental compatibility as novel pesticide computationally identified candidates. For herbicidal-likeness, compounds were required to possess moderate molecular weight (150–500 Da), balanced lipophilicity (iLogP ≤ 3.5), TPSA ≤ 100 Å², HBD ≤ 3, HBA ≤ 12, and RBs ≤ 12. Based on these criteria, 61 of the 140 compounds satisfied the herbicidal profile, comprising 15 chrysin, 13 apigenin, 29 naringenin, 2 hesperetin, and 2 quercetin derivatives. The insecticidal screening criteria emphasized suitable permeability and interaction with neural targets, including MW ≤ 500 Da, iLogP between 0 and 5, TPSA ≤ 100 Å², HBD ≤ 2, HBA between 1 and 8, and RBs ≤ 12. A total of 66 compounds met these requirements, including 22 chrysin, 16 apigenin, 24 naringenin, and 4 quercetin derivatives. For fungicidal-likeness, the physicochemical requirements were MW ≤ 500 Da, iLogP between 1.5 and 5.0, TPSA of 60–130 Å², HBD ≤ 3, HBA ≤ 7, and RBs ≤ 9, reflecting the characteristics required for effective interaction with the succinate dehydrogenase binding pocket. Under these criteria, 96 compounds were retained, including 24 chrysin, 17 apigenin, 38 naringenin, 13 hesperetin, and 2 quercetin derivatives. In contrast, all 140 derivatives fulfilled the criteria established for both molluscicidal- and larvicidal-likeness. These profiles permitted broader physicochemical ranges, particularly for polarity and hydrogen-bonding capacity, indicating that the entire flavonoid library possesses structural features compatible with the respective biological targets.

Table 2. Physicochemical criteria for herbicide-, insecticide-, fungicide-, molluscicidal- and larvicidal-likeness.

Property	H	I	F	M	L
MW(Da)	150-500 better permeability and binding	150-500 ensures good penetration	≤ 500 ensures good diffusion and fitting	≤ 500 allows flavonoid to fit into the deep and narrow AChE gorge.	≤ 500 ensures flavonoids can fit into the hydrophobic hormone-binding cavity.
iLog P	≤ 3.5 ensures balanced hydrophobicity and aqueous solubility	0-5 required for hydrophobic interactions with aromatic residues	1.5-5.0 slightly higher lipophilicity preferred for hydrophobic SDH pocket	2.5–5.0 moderate lipophilicity required for π–π stacking with aromatic residues	2.0-5.0 hydrophobic JHBP pocket requires moderately lipophilic compounds
TPSA (Å²)	≤100 good interaction with protein	≤ 100 high polarity reduces ability to cross into neural sites	60-130 adequate polarity for binding	≤ 140 too high polarity prevents penetration into hydrophobic gorge	≤ 140 lower TPSA improves penetration and binding in hydrophobic environment.
HBD	≤ 3 maintains stable H-bonds with active residues	≤ 2 prevents excess polarity; helps stable H-bonding with catalytic triad residues.	≤ 3 maintains stable H-bonds with key residues without excessive polarity	≤ 5 prevents excessive polarity; ensures stable H-bonds with catalytic triad	≤ 5 allows H-bonding with key residues without excess polarity.
HBA	≤12 maintains stable H-bonds with active residues	1-8 maintains favourable H-bonding without reducing lipophilicity	≤ 7 balanced polarity for strong interactions with SDH residues	≤ 10 maintains balanced polarity for interaction with gorge residues.	≤ 10 maintains good polarity balance for stable interaction.
RBs	≤ 12 ensures flavonoid does not lose affinity due to excessive conformational freedom	≤ 12 prevents loss of affinity	≤ 9 ensures conformational stability inside the binding site.	-	-
No. of screened compounds/ Total no. of compounds	61/140	66/140	96/140	140/140	140/140

Filter 1 clearly shows that every compound in the dataset had potential molluscicidal and larvicidal activity, while herbicidal and insecticidal likeness were more restricted, and fungicidal activity was intermediate. All the 140 flavonoid derivatives and reference compounds obey Lipinski rule.

Based on docking scores, the screened compounds appear to exhibit higher affinity toward the target proteins compared to the reference compounds. The multi-target docking evaluation of flavonoid derivatives revealed distinct structure activity trends across herbicidal, insecticidal, fungicidal, molluscicidal, and larvicidal endpoints (**Table 3)**. For herbicidal activity, promising retention was observed in Apigenin-IIa, Chrysin-Ia/Ib2, and Naringenin-IIIa/IIIb, with binding energies comparable to the reference herbicide Imazapyr, while hesperetin derivatives were largely

excluded due to physicochemical or docking constraints. In insecticidal screening, strong activity was confined to Chrysin subgroups (Ib1, Ib2, Ic, Id), Apigenin-IIa, and Naringenin-IIIa, which matched or outperformed the natural insecticide Karanjin, whereas hesperetin and quercetin derivatives proved unsuitable. For fungicidal potential, multiple scaffolds showed robust retention, notably Chrysin (Ib1–Ib3, Id, Ie), Apigenin (IIa, IIb), Naringenin (IIIa–IIIc), and Hesperetin (IVb1, IVb2, IVc1), with binding affinities frequently surpassing the natural fungicide Cnidiadin, supporting their candidacy as antifungal computationally identified candidates. Molluscicidal screening revealed the broadest activity spectrum, with nearly universal retention across flavonoid classes. The Hesperetin (IVb1, IVb2, IVc1, IVc2) derivatives were the most potent, followed by Naringenin (IIIb, IIIc) Apigenin (IIb) and Chrysin (Ib2, Ib3), all exceeding the binding strength of the reference molluscicide Niclosamide. Finally, larvicidal evaluation demonstrated consistently high activity across scaffolds. Hesperetin derivatives emerged as the strongest candidates, while Chrysin (Ib3) also provided highly potent binders. Even quercetin derivatives, though partially excluded, contributed moderately active members. Binding scores frequently outperformed the standard larvicide Methoprene, positioning flavonoids as strong contenders for next-generation larvicidal agents. In summary, flavonoid scaffolds display multi-target agrochemical potential, with Chrysin, Naringenin, and Hesperetin derivatives consistently dominating across insecticidal, fungicidal, molluscicidal, and larvicidal endpoints, while Apigenin-IIa remains a reliable herbicidal candidate. These results highlight flavonoids as versatile scaffolds for the development of eco-friendly, broad-spectrum agrochemicals. The reference compounds, Imazapyr (H, BE -5.57 kcal/mol), Karanjin (I, BE -7.31 kcal/mol), Cnidiadin (F, BE -5.80 kcal/mol), Niclosamide (M, BE -7.94 kcal/mol) and Methoprene (L, BE -5.98 kcal/mol) were included for efficacy comparison, despite exhibiting certain deviations from the ideal ADMET parameters.

Table 3. Docking outcomes of Flavonoid derivatives: Binding affinities and active ratios across agrochemical targets.

Group Name	G. No.	UPO (H*)	GABA (I*)	SDH (F*)	AChE (M*)	JHBP (L*)
Chrysin Derivatives	Ia	-5.09 to -8.06 (9/10)	-5.82 to -7.87 (5/10)	-5.67 to -7.39 (7/11)	-6.65 to -8.63 (13/13)	-6.3 to -8.2 (10/13)
	Ib1	-	-6.94 to -8.14 (3/3)	-7.66 to -8.03 (3/3)	-8.98 to -9.15 (3/3)	-8.03 to -8.44 (3/3)
	Ib2	-8.19 to -8.65 (2/2)	-7.47 to -8.56 (3/3)	-7.68 to -8.87 (4/4)	-9.23 to -9.69 (4/4)	-8.46 to -8.72 (4/4)
	Ib3	-	-	-8.32 (1/1)	-10.07 to -10.46 (3/3)	-8.71 to -10.04 (3/3)
	Ic	-	-6.92 to -8.58 (3/3)	-6.39 (0/1)	-8.92 to -9.47 (3/3)	-8.71 to 8.82 (3/3)
	Id	-6.1 to -6.41 (0/3)	-7.55 to-7.67 (3/3)	-7.78 to -8.78 (3/3)	-8.09 to -8.23 (3/3)	-7.02 to -7.18 (3/3)
	Ie	-	-	-8.12 (1/1)	-8.12 (1/1)	-8.97 (1/1)
Apigenin Derivatives	IIa	-5.44 to -8.53 (12/13)	-5.58 to -8.34 (8/16)	-6.35 to -7.75 (14/16)	-6.74 to -9.3 (17/17)	-5.49 to -8.27 (14/17)
	IIb	-	-	-7.31 (1/1)	-10.23 to -10.38 (3/3)	-5.74 to -8.63 (1/3)
Naringenin Derivatives	IIIa	-4.54 to -8.48 (10/16)	-5.4 to -7.55 (13/19)	-5.76 to -7.76 (15/19)	-6.85 to -9.76 (19/19)	-5.78 to -7.79 (17/19)
	IIIb	-6.2 to -8.43 (6/8)	-5.83 to -7.36 (3/5)	-6.02 to -7.99 (10/11)	-7.63 to -10.19 (11/11)	-5.63 to -8 (9/11)
	IIIc	-6.1 to -7.26 (1/5)	-	-6.08 to -8.68 (6/8)	-8.72 to -10.53 (12/12)	-7.14 to -8.51 (12/12)
Hesperetin Derivatives	IVa1	-5.06 to -5.72 (0/5)	-	-5.67 to -5.13 (0/5)	-8.54 to -9.74 (5/5)	-7.07 to -8.16 (5/5)
	IVa2	-	-	-	-8.9 to -9.43 (4/4)	-7.35 to -8.38 (4/4)
	IVb1	-	-	-7.76 to -8.53 (3/3)	-10.04 to -11.27 (9/9)	-8.6 to -9.95 (9/9)
	IVb2	-	-	-8.46 to 8.8 (4/4)	-10.43 to -12.37 (7/7)	-8.63 to -10.29 (7/7)
	IVc1	-	-	-6.85 to -9.17 (4/4)	-9.85 to -11.67 (8/8)	-7.67 to -9.33 (8/8)
	IVc2	-	-	-	-10.24 to -11.41 (3/3)	-9.1 to -10.53 (3/3)
Quercetin Derivatives	V	-6.73 to -7.26 (2/2)	-5.51 to -6.44 (0/4)	-5.22 to -5.97 (0/4)	-6.67 to -10.27 (12/12)	-5.66 to -8.9 (9/12)
Reference compounds		Imazapyr -5.57	Karanjin -7.31	Cnidiadin -5.80	Niclosamide -7.94	Methoprene -5.98

B.E -Minimum to maximum binding energy range, the ratio between the number of compounds filtered from filter 1 with number of compound having binding energy greater than -7 kcal/mol, G.No.-Group number, H*-Herbicidal likeness, I*-Insecticidal likeness, F*-Fungicidal likeness, M*-Molluscicidal likeness, L*-Larvicidal likene

The In-silico safety assessment of flavonoid scaffolds revealed an overall favourable profile across metabolic and toxicity endpoints, though scaffold-specific variations were evident (**Table S7-S12**). Regarding CYP2D6 inhibition, most scaffolds were largely non-inhibitory, with groups Ib1, Ib3, Ic, Id, Ie, IIa, IVa2, IVb1, IVc2, and V showing complete absence of inhibition, indicating minimal metabolic liability, while subgroup Ia showed moderate inhibition. AMES mutagenicity predictions demonstrated that the majority of scaffolds were non-mutagenic, with Ib1, Ib2, Ic, Id, Ie, IVa2, IVb1, IVb2, IVc1, IVc2, and V

displaying 100% non-mutagenicity, whereas Ia had approximately one-third of compounds flagged for mutagenicity. For non-carcinogenicity, similar trends were observed, subgroups Ib2, Ib3, Ic, Ie, IIb, IIIa, IIIb, IVa–c, and V were predominantly non-carcinogenic, while Ia exhibited moderate concern. Non-hepatotoxicity assessment indicated that Ib1, Ib2, Ic, Id, Ie, and group V were largely safe, with IIa, IIIa, IIIb, and subgroup IIIc showing some hepatotoxicity in specific members. In skin sensitization, subgroups Ib2, Ic, Id, Ie, IIIa, IIIb, and IVa–c was consistently non-sensitizing, whereas Ia, IIa, IIb, and IIIc had variable responses. Eye irritation predictions showed that Ic, Id, Ie, IIIb, and IVa–c were highly safe, while Ia, IIa, and IIIc exhibited partial liability. Finally, hERG liability analysis highlighted that Ib1, Ib3, Ic, Id, Ie, IIIb, and IVb1/IVb2 were highly safe, with moderate risk in IIa, IIIa, IIIc, and V scaffolds. Overall, the integrated analysis identifies scaffolds Ic, Id, Ie, IIIb, IVa–c, and V as the most promising in terms of broad-spectrum safety, consistently performing well across CYP2D6, mutagenicity, carcinogenicity, hepatotoxicity, skin sensitization, eye irritation, and cardiotoxicity endpoints. This comprehensive evaluation underscores the potential of specific flavonoid chemotypes as safe potential candidates with minimal metabolic and toxicological liabilities. Bioaccumulation is an important environmental parameter for agrochemical development because compounds that accumulate in aquatic organisms may pose long-term ecological risks. According to common regulatory interpretations, compounds with Bioaccumulation factor (BAF) values below 1000 are generally considered to have low bioaccumulation potential. In the present study, 132 of the 140 flavonoid derivatives (94.3%) showed predicted BAF values below 1000 (**Table S18**), suggesting a generally low bioaccumulation tendency. This favourable profile may be attributed to the balanced physicochemical properties of the flavonoid scaffold, including moderate molecular weight, polarity, and hydrogen-bonding capacity. The compounds with BAF values above 1000 () indicates that structural modifications leading to excessive lipophilicity. Overall, the results suggest that most of the screened flavonoid derivatives possess acceptable environmental behaviour and are unlikely to present significant bioaccumulation concerns.

Table 4. Distribution of Flavonoids Derivatives Across Physicochemical, Docking and ADMET/Safety Filters.

Group Name	G. No.	H*			I*			F*			M*			L*		
		F1	F2	F3	F1	F2	F3	F1	F2	F3	F1	F2	F3	F1	F2	F3
Chrysin Derivatives	Ia	10/13	9/10	4/9	10/13	5/10	3/5	11/13	7/11	2/7	13/13	13/13	4/13	13/13	10/13	4/10
	Ib1	-	-	-	3/3	3/3	-	3/3	3/3	-	3/3	3/3	-	3/3	3/3	-
	Ib2	2/4	2/2	-	3/4	3/3	-	4/4	4/4	-	4/4	4/4	-	4/4	4/4	-
	Ib3	-	-	-	-	-	-	1/3	1/1	1/1	3/3	3/3	1/3	3/3	3/3	1/3
	Ic	-	-	-	3/3	3/3	-	1/3	0/1	-	3/3	3/3	-	3/3	3/3	-
	Id	3/3	0/3	-	3/3	3/3	-	3/3	3/3	-	3/3	3/3	-	3/3	3/3	-
	Ie	-	-	-	-	-	-	1/1	1/1	-	1/1	1/1	-	1/1	1/1	-
Apigenin Derivatives	IIa	13/17	12/13	1/12	16/17	8/16	1/8	16/17	14/16	2/14	17/17	17/17	2/17	17/17	14/17	2/14
	IIb	-	-	-	-	-	-	1/3	1/1	-	3/3	3/3	1/3	3/3	1/3	1/1
Naringenin Derivatives	IIIa	16/19	10/16	1/10	19/19	13/19	2/13	19/19	15/19	2/15	19/19	19/19	2/19	19/19	17/19	2/17
	IIIb	8/11	6/8	3/6	5/11	3/5	-	11/11	10/11	3/10	11/11	11/11	3/11	11/11	9/11	3/9
	IIIc	5/12	1/5	-	-	-	-	8/12	6/8	-	12/12	12/12	-	12/12	12/12	-
Hesperetin Derivatives	IVa1	2/5	0/5	-	-	-	-	2/5	0/5	-	5/5	5/5	-	5/5	5/5	-
	IVa2	-	-	-	-	-	-	-	-	-	4/4	4/4	-	4/4	4/4	-
	IVb1	-	-	-	-	-	-	3/9	3/3	-	9/9	9/9	-	9/9	9/9	-
	IVb2	-	-	-	-	-	-	4/7	4/4	-	7/7	7/7	-	7/7	7/7	-
	IVc1	-	-	-	-	-	-	4/8	4/4	1/4	8/8	8/8	1/8	8/8	8/8	1/8
	IVc2	-	-	-	-	-	-	-	-	-	3/3	3/3	1/3	3/3	3/3	1/3
Quercetin Derivatives	V	2/12	2/2	1/2	4/12	0/4	-	4/12	0/4	-	12/12	9/12	1/9	12/12	9/12	1/9
Total		61	42	10	66	41	6	96	76	11	140	140	16	140	125	16

G.No.-Group number, H*-Herbicidal likeness, I*-Insecticidal likeness, F*-Fungicidal likeness, M*-Molluscicidal likeness, L*-Larvicidal likeness, F1-Filter based on physicochemical properties, F2-Filter based on docking score ≥-7 kcal/mol, F3-Filter based on ADMET and safety profiles.

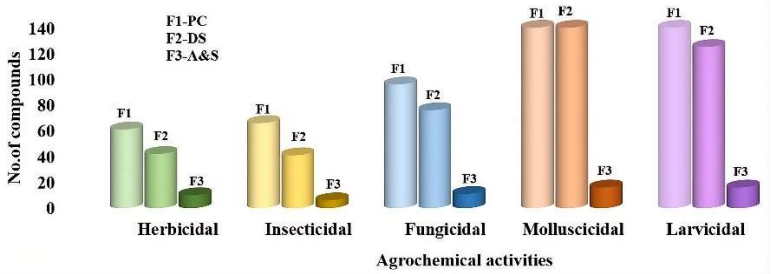

Figure 2. Three-Stage Filtering of Flavonoid derivatives Across Agrochemical Activities.

Outcome of the Three-Filter Screening

Overall, across all five agrochemical activities, the ADMET/safety filter (F3) was the main limiting factor. Scaffolds consistently crossing F3, Chrysin Ia, Naringenin IIIa/b, Apigenin IIa, and Quercetin V, represent the most robust computationally identified candidates for multi-activity agrochemical development. Based on the integrated screening results, 16 active derivatives were identified across flavonoid subgroups and advanced for detailed SAR evaluation (**Table 4-5, S13-17, Figure 2-3**).

Table 5. Summary of Docking results and ADMET evaluation of screened compounds across target proteins.

	H	I	F	M	L
1*	61	66	96	140	140
2*	UPO	GABA	SDH	AChE	JHBP
3*	-4.54 to -8.65	-5.40 to -8.58	-5.13 to -9.17	-5.66 to -12.37	-5.49 to -10.53
4*	42	41	76	140	125
5*	Ib2	Ic	IVc1	IVb2	IVc2
6*	10 (Ia, IIa, IIIb, and V)	6 (Ia, IIa and IIIa)	11 (Ia, Ib3, IIa, IIIa, IIIb, and IVc1)	16 (Ia, Ib3, IIa, IIb, IIIa, IIIb, IVc1, IVc2 and V)	16 (Ia, Ib3, IIa, IIb, IIIa, IIIb, IVc1, IVc2 and V)

1*No. of screened compounds; 2* Protein Target; 3* BE (kcal/mol); 4* No. of compounds passing docking cutoff (BE ≥-6.45 kcal/mol); 5* Group with peak performance in docking studies; 6* No. of compounds with acceptable ADMET parameters and favorable safety profile.

Table 6. Group-wise distribution of active derivatives chosen as templates based on pesticidal potential.

Groups	Chrysin Derivatives		Apigenin Derivatives		Naringenin Derivatives		Hesperetin Derivatives		Quercetin Derivatives
Activity	Group Ia	Group Ib3	Group IIa	Group IIb	Group IIIa	Group IIIb	Group IVc1	Group IVc2	Group V
H	2-4, 11	-	46	-	59	73,75,78	-	-	136
I	2-4	-	46	-	59,65	-	-	-	-
F	3,4	21	36,46	-	59,65	73,75,78	119	-	-
M	2-4, 11	21	36,46	50	59,65	73,75,78	119	126	136
L	2-4, 11	21	36,46	50	59,65	73,75,78	119	126	136

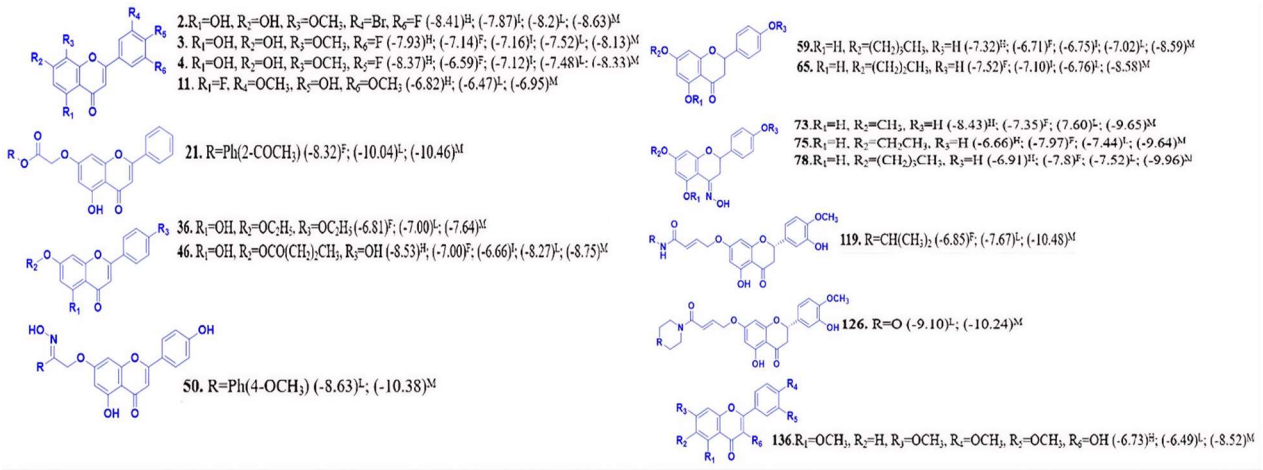

Figure 3. Active flavonoid derivatives and associated binding energies.

Structure Activity relationship

The Chrysin (Ia) series yielded four derivatives (**2**, **3**, **4**, and **11**) that passed all three screening filters, identifying them as the most promising candidates for SAR analysis. Among these, compound **2** exhibited the strongest multi-target docking performance, supported by multiple hydrogen bonds, halogen contacts and π–π stacking interactions. The presence of both bromine and fluorine appears to enhance binding through increased hydrophobic complementarity and stabilization of aromatic interactions. Compound **3** (**Figure 4**, **Table 8**) retained strong activity across all evaluated targets, indicating

that fluorination at the R_6 position is sufficient to maintain activity, while the additional bromine substituent in compound **2** further improves potency. Compound **4** showed favourable herbicidal and molluscicidal binding but lower fungicidal activity, suggesting that relocating fluorine from R_6 to R_5 alters its orientation and reduces favourable halogen-bonding interactions. In contrast, compound **11** displayed weaker binding, indicating that bulky O-alkyl substitution may compromise activity by disrupting the balance between lipophilicity and hydrogen-bonding capacity. Overall, dual halogenation, particularly the Br/F combination, promotes target binding, whereas free phenolic hydroxyl groups at R_1 and R_2 remain essential for hydrogen-bond anchoring. These observations identify compound **2** as the most promising candidate within this series.

Within the Ib3 subgroup, compound **21** (**Figure 4**, **Table 8**) demonstrated selective pesticidal activity with strong fungicidal, larvicidal, and molluscicidal affinities. Its activity is largely attributed to the ortho-acetylphenyl substituent, which enhances aromatic interactions and facilitates additional hydrogen-bonding and electrostatic contacts. The combination of π-stacking, π-cation/anion interactions, and favorable polar contacts likely contributes to its strong target-specific binding.

Among the II-series derivatives, compound **46** (IIa) (**Figure 4**, **Table 8**) emerged as the best multi-target binder. Its superior activity can be attributed to the presence of two phenolic hydroxyl groups that provide strong hydrogen-bonding interactions and a bulky lipophilic ester substituent that enhances hydrophobic and π-type contacts within the binding pockets. Compound **36** retained moderate fungicidal and molluscicidal activity but exhibited weaker herbicidal binding. The reduced performance may result from O-alkylation at R_2 and R_3, which decreases hydrogen-bond donor capacity and shifts the interaction profile toward weaker hydrophobic and lone-pair interactions. In the IIb series, compound **50** displayed strong larvicidal and molluscicidal activity. The para-methoxy substituent increases electron density on the aromatic ring, promoting π–π stacking, π–alkyl interactions, and additional hydrogen-bonding contacts that collectively enhance binding affinity.

The III-series compounds highlight the importance of alkyl chain length in modulating activity. Compounds **59** (n-butyl) and **65** (n-propyl) exhibited strong molluscicidal activity, primarily driven by hydrophobic and π–alkyl interactions, while conserved hydrogen-bonding interactions from the flavonoid core provided additional stabilization. The slightly improved fungicidal and insecticidal activity of compound **65** suggests that the shorter propyl chain achieves a better fit within these target pockets. A similar trend was observed in the IIIb subgroup, where compound **73** (methyl substitution) showed the strongest herbicidal activity through efficient hydrogen bonding and π–π stacking. Increasing alkyl chain length from ethyl (**75**) to butyl (**78**) generally maintained or enhanced molluscicidal activity but reduced herbicidal potency, indicating that hydrophobic substituents

preferentially favour molluscicidal target interactions.

Compounds from the IV-series displayed pronounced molluscicidal selectivity. Compound **119** (IVc1) (**Figure 4**, **Table 8**) achieved excellent molluscicidal affinity due to its branched isopropyl substituent, which acts as a compact hydrophobic group capable of maximizing alkyl and π–alkyl contacts while preserving key hydrogen-bonding interactions from the flavonoid core. Similarly, compound **126** (IVc2) showed exceptional molluscicidal activity through a combination of strong hydrogen-bonding interactions, carbonyl-mediated contacts, and extensive π-cation and π-stacking interactions. These features also supported favourable larvicidal binding.

Compound **136** (V) displayed selective affinity toward the molluscicidal target. Its activity appears to arise from the combined effects of multiple methoxy substituents and a phenolic hydroxyl group, which collectively promote hydrogen bonding, hydrophobic interactions, and aromatic stabilization. These findings suggest that electron-rich substituents play an important role in enhancing target specificity and binding strength. The key protein–ligand interactions of the representative compounds are summarized in **Table 8**.

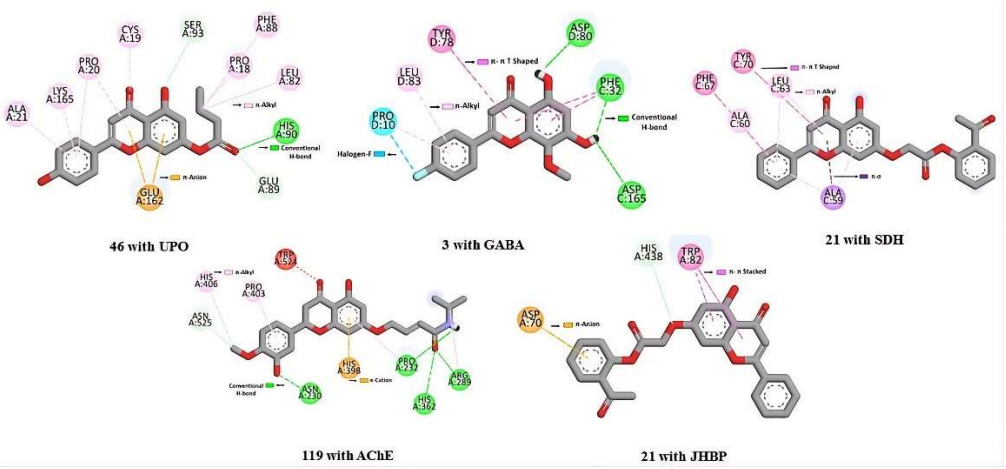

Figure 4. Interactions of some representative top computationally identified candidates within the active site of the proteins.

Table 8. Key protein–ligand interactions of the potential flavonoid derivatives with their respective agrochemical targets.

Compound	Target protein	Amino acid residues	Interaction tSype
46	UPO (Herbicidal target)	His90, Glu89	Conventional H-bond
		Glu162	π-Anion
		Ala21, Lys165, Pro20, Cys19, Phe88, Pro18, Leu82	π-Alkyl
3	GABA receptor (Insecticidal target)	Asp80, Phe32, Asp165	Conventional H-bond
		Pro10	Halogen bond (F)
		Leu83, Pro10	π-Alkyl
		Tyr78, Phe32	π–π T-shaped
21	SDH (Fungicidal target)	Phe67, Tyr70	π–π T-shaped
		Ala59, Ala60, Leu63	π-Alkyl
		Ala59	π-σ
119	AChE (Molluscicidal target)	Asn230, Pro232, His362, Arg289	Conventional H-bond
		His406, Pro403, Pro232, Arg289	π-Alkyl
		His398	π-Cation
21	JHBP (Larvicidal target)	Asp70	π-Anion
		Trp82	π–π Stacked

Overall, compounds **3**, **4**, **46**, and **59** demonstrated favourable binding across multiple agrochemical targets, highlighting their potential as broad-spectrum flavonoid-based candidates. Their activities are supported by a balanced combination of hydrogen bonding, π–π stacking, π–alkyl interactions, and hydrophobic contacts. In contrast, several compounds displayed clear target selectivity. Compound **46** showed the strongest herbicidal activity, compound **2** emerged as the most promising insecticidal candidate, compound **21** exhibited the highest fungicidal and larvicidal potential, and compound **119** displayed the greatest molluscicidal affinity. Together, these results demonstrate that subtle modifications in flavonoid substitution patterns can be exploited to achieve either broad-spectrum activity or target-specific selectivity, providing valuable guidance for the rational design of next-generation agrochemical candidate.

Molecular Dynamics Simulation

In the AChE system, **21** exhibited a sustained hydrogen-bonding pattern, with 1–2 hydrogen bonds maintained consistently during the latter half of the simulation (≈10–22 ns). This persistent H-bond formation indicates stable ligand anchoring within the active site [26]. In contrast, the reference compound niclosamide showed more fluctuating hydrogen bond interactions, with intermittent formation and loss over the simulation period, suggesting comparatively lower interaction stability. In the UPO system, **46** demonstrated stable hydrogen bond formation during the early and mid-phases of the simulation, whereas the reference imazapyr displayed higher variability with frequent spikes and drops in hydrogen bond numbers. Although imazapyr formed occasional multiple hydrogen bonds, their transient nature indicates weaker long-term stabilization (**Figure 5**).

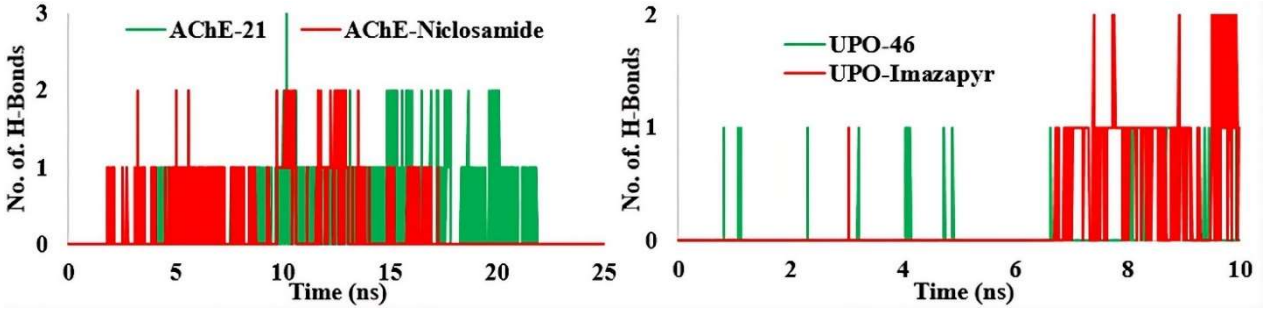

Figure 5. Time-dependent hydrogen bond analysis.

The AChE–**21** complex displayed a relatively stable SASA profile throughout the 25 ns simulation, fluctuating narrowly around ~220–230 nm². This behaviour was comparable to the reference AChE–niclosamide complex, suggesting that **21** maintains a compact and well-stabilized protein conformation. The absence of significant SASA deviations indicates limited unfolding or surface exposure, supporting strong and stable binding. Similarly, the UPO–**46** complex exhibited consistent SASA values (~210–220 nm²) over the 10 ns simulation, closely matching those of the reference UPO–imazapyr complex. Minor fluctuations observed in both systems reflect natural protein flexibility rather than destabilization (**Figure 6**).

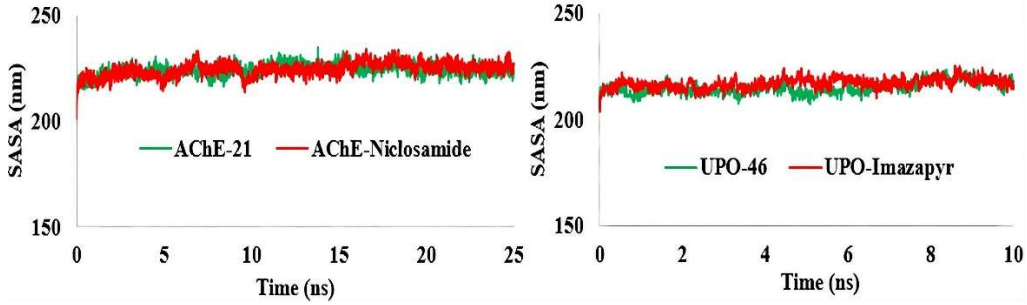

Figure 6. SASA trajectories.

The AChE–**21** complex exhibited uniformly low RMSF values across most residues, indicating minimal local fluctuations. This profile closely overlapped with that of the reference AChE–niclosamide complex, suggesting that compound **21** stabilizes the protein structure to an extent comparable with the known inhibitor. Minor peaks observed at terminal and loop regions are typical of flexible segments and do not indicate structural destabilization. In contrast, the UPO-**46** complex demonstrated significantly lower RMSF values cross the entire residue range compared to the reference UPO–imazapyr complex. This marked reduction in flexibility indicates that **46** effectively restricts residue motion and induces a more rigid and stable binding environment (**Figure 7**).

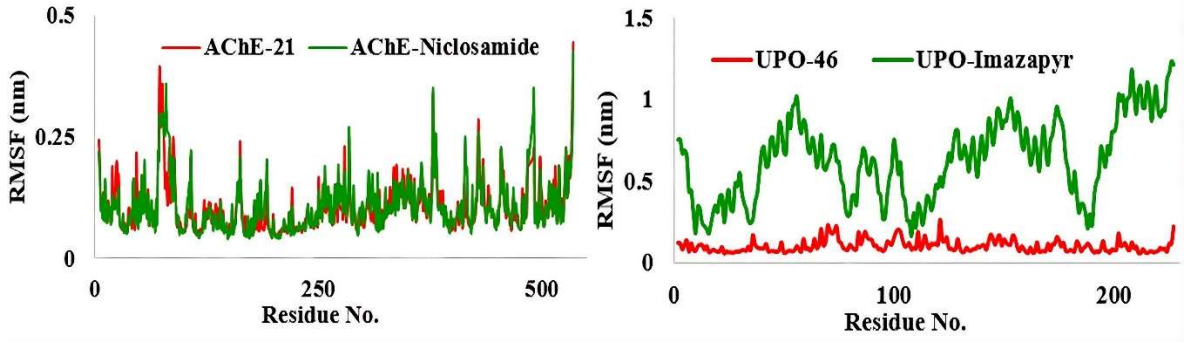

Figure 7. RMSF profiles.

The AChE–**21** complex rapidly equilibrated within the initial phase of the simulation and maintained a stable RMSD throughout the 25 ns trajectory. In comparison, the reference AChE–niclosamide complex exhibited higher RMSD values and greater fluctuations, particularly after 10 ns, suggesting increased conformational flexibility. The relatively lower and stable RMSD of AChE–**21** indicates a more stable protein–ligand complex. Similarly, the UPO–**46** complex achieved early stabilization within the first nanosecond and maintained consistent RMSD values around 7–8 nm across the 10 ns simulation. Although the reference UPO–imazapyr complex also displayed stable behaviour, it showed intermittent fluctuations, whereas compound **46** demonstrated smoother RMSD convergence (**Figure 8**).

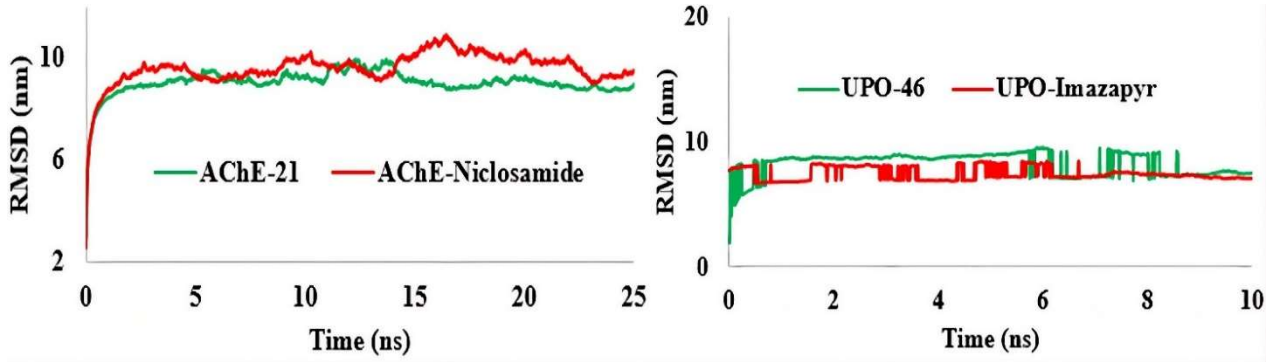

Figure 8. RMSD analysis.

Both the AChE–**21** complex and the reference AChE–niclosamide complex maintained highly stable Rg values throughout the 25 ns simulation. The close overlap between the two trajectories suggests that binding of **21** preserves the global structural integrity of AChE to a degree comparable with the commercial reference. The UPO–**46** complex also displayed a stable Rg profile across the 10 ns simulation, indicating sustained compactness of the protein structure. Although the reference UPO–imazapyr complex exhibited a brief spike in Rg toward the end of the simulation, the overall profile remained stable, while **46** showed a smoother and more consistent trajectory (**Figure 9**).

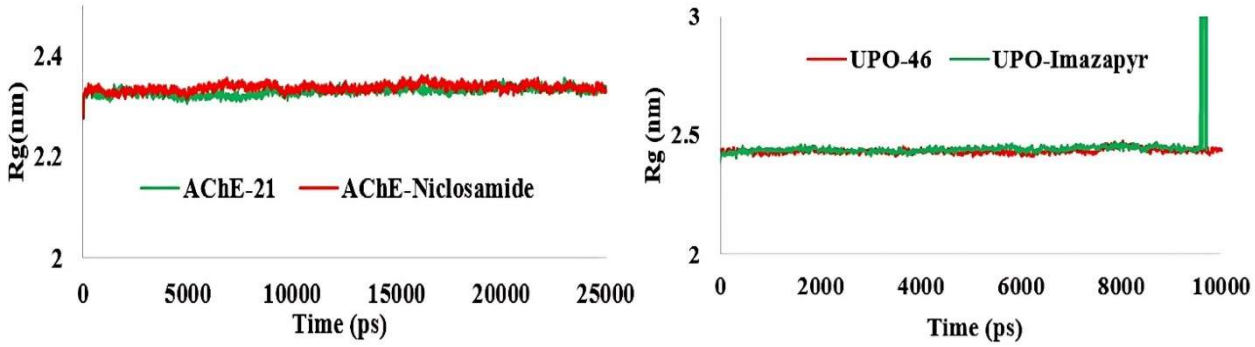

Figure 9. Radius of gyration plots.

The combined electrostatic and van der Waals energy profiles indicate that **46** forms a more energetically stable complex with UPO than the reference herbicide imazapyr. Similarly, **21** establishes a more energetically stable binding network with AChE than niclosamide (**Figure 10**). These stable interaction energies corroborate the docking and structural stability results, further supporting **46** as a robust and dynamically stable agrochemical potential agrochemical candidates and **21** as a promising insecticidal potential agrochemical candidate.

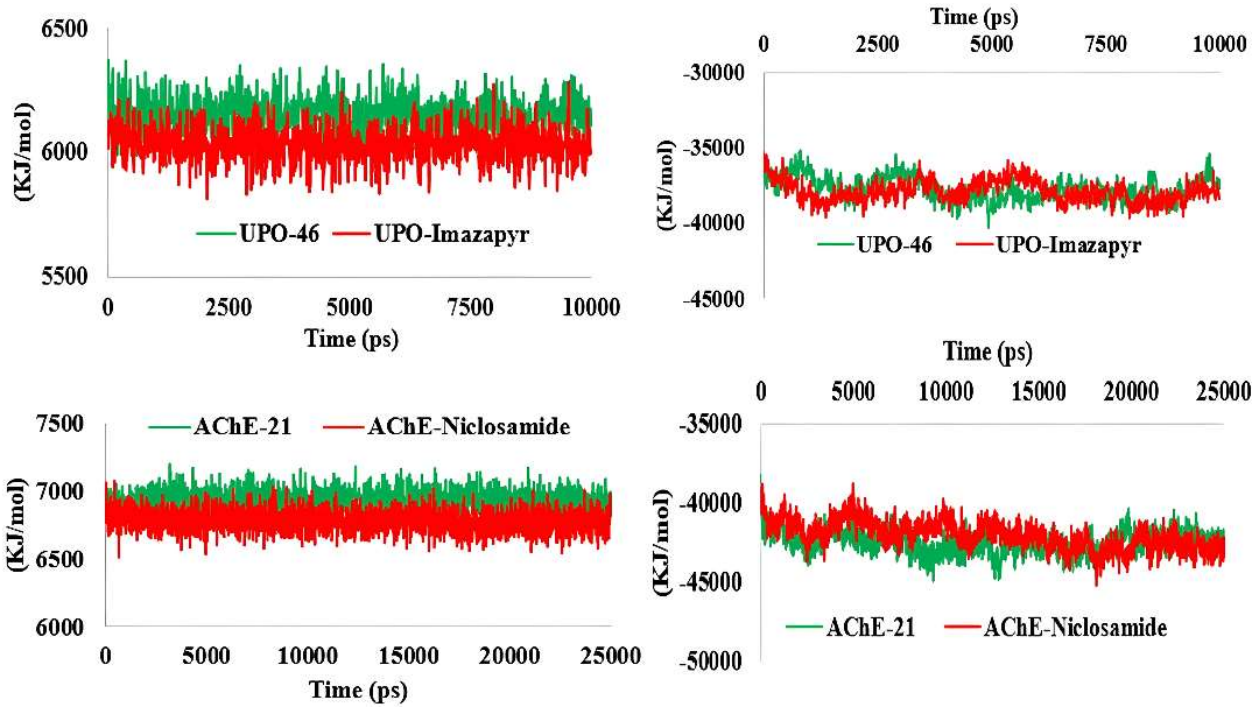

Figure 10. Short-range Coulombic interaction energy and Lennard-Jones Interaction.

Conclusion

This study provides a comprehensive computational assessment of 140 flavonoid derivatives from five major subgroups for their potential as eco-friendly agrochemicals. A three-tier screening strategy effectively narrowed down the large dataset to a set of robust candidates. The results highlight that while molluscicidal and larvicidal potential was broadly distributed across the dataset, herbicidal and insecticidal activities were more restricted, and fungicidal activity was intermediate. Scaffolds consistently passing F3, Chrysin Ia, Naringenin IIIa/b, Apigenin IIa, and Quercetin V, emerged as the most robust multi-activity computationally identified candidates. Overall, 16 active derivatives were identified for detailed SAR analysis. Molecular dynamics simulations

validated the robustness of the selected flavonoid–target complexes, confirming stable binding, preserved protein compactness, and favourable interaction energetics, thereby reinforcing their potential as effective and sustainable potential agrochemical candidates. Overall, this integrative workflow demonstrates that flavonoid scaffolds represent versatile and safe chemotypes with both broad-spectrum and target-specific potential, offering a rational framework for the design and optimization of next-generation sustainable agrochemicals.

Supplementary file

Detailed results, including Supplementary Tables and Figures are provided in the Supplementary Information.

References

[1] Pereira V, Figueira O, Castilho P. Flavonoids as Insecticides in Crop Protection—A Review of Current Research and Future Prospects. Plants 2024;13(6):776.

[2] Schnarr L, Segatto M, Olsson O, Zuin V, Kümmerer K. Flavonoids as biopesticides – Systematic assessment of sources, structures, activities and environmental fate. Science of The Total Environment 2022;824:153781.

[3] Zhang Y, Wang X, Bian Z, Se C, Yang G, Lu Y. Application of flavonoid compounds suppresses the cotton aphid, Aphis gossypii. Frontiers in Plant Science 2025;16:1545499.

[4] Javaid A, Shafique S, Kanwal Q, Shafique S. Herbicidal activity of flavonoids of mango leaves against Parthenium hysterophorusL. Natural Product Research 2010;24(19):1865-1875.

[5] Inaba K, Ebihara K, Senda M, Yoshino R, Sakuma C, Koiwai K, Takaya D, Watanabe C, Watanabe A, Kawashima Y, Fukuzawa K, Imamura R, Kojima H, Okabe T, Uemura N, Kasai S, Kanuka H, Nishimura T, Watanabe K, Inoue H, Fujikawa Y, Honma T, Hirokawa T, Senda T, Niwa R. Molecular action of larvicidal flavonoids on ecdysteroidogenic glutathione S-transferase Nopperabo in Aedes aegypti. BMC Biology 2022;20(1):43.

[6] Singaba A, Ahmed A, Sinkkonen J, Ovcharenko V, Pihlaja K. Molluscicidal Activity and New Flavonoids from Egyptian Iris germanica L. (var. alba). Zeitschrift für Naturforschung C 2006;61(1-2):57-63.

[7] Li A, Zhao Z, Zhang S, Zhang Z, Shi Y. Fungicidal Activity and Mechanism of Action of Glabridin from Glycyrrhiza glabra L. International Journal of Molecular Sciences 2021;22(20):10966.

[8] Gruseck R, Hofmann T, Zumstein M. Flavonoid Stability and Biotransformation in Agricultural Soils: Effects of Hydroxylation, Methoxylation, and Glycosylation. Journal of Agricultural and Food Chemistry 2025;73(23):14245-14252.

[9] Goławska S, Sprawka I, Łukasik I, Goławski A. Are naringenin and quercetin useful chemicals in pest-management strategies?. Journal of Pest Science 2013;87(1):173-180.

[10] Divya D, Kalpana A. In-Silico Analysis of Coumarins for Neurodegenerative, Infectious and Metabolic Diseases. French-Ukrainian Journal of Chemistry 2025;13(1):79-97.

[11] Yıldırır Y, Özel S, Doyduk D, Kartal Y, Sabuncuoğlu S. Synthesis of Apigenin and Quercetin-Like Compounds, Molecular Docking Simulation, and Investigation of Their Bioactivity on A549 Cell Lines. ChemistrySelect 2022;7(43):e202203121.

[12] He B, Fan X, Zheng T, Gao Y, Chen X, Liu Y, Zhang Y. Design, Synthesis, and Biological Evaluation of Novel Apigenin Derivatives as Potential Antitumor Agents. Russian Journal of Bioorganic Chemistry 2024;50(5):1659-1671.

[13] Liu S, Zheng X, Luo Z, Tang C, Hu Y, Peng Q, Mi P, Chen H, Yao X. The synthesis and bioactivity of apigenin derivatives. Fitoterapia 2024;179:106228.

[14] Wang Q, Shi J, Chen C, Huang C, Tang W, Li J. Hesperetin derivatives: Synthesis and anti-inflammatory activity. Bioorganic & Medicinal Chemistry Letters 2016;26(5):1460-1465.

[15] Ding H, Huang A, Zhang Y, Li B, Huang C, Ma T, Meng X, Li J. Design, synthesis and biological

evaluation of hesperetin derivatives as potent anti-inflammatory agent. Fitoterapia 2017;121:212-222.

[16] Li X, Cai Y, Yang F, Meng Q. Synthesis and molecular docking studies of chrysin derivatives as antibacterial agents. Medicinal Chemistry Research 2017;26(10):2225-2234.

[17] Imran S, Taha M, Ismail N, Kashif S, Rahim F, Jamil W, Hariono M, Yusuf M, Wahab H. Synthesis of novel flavone hydrazones: In-vitro evaluation of α-glucosidase inhibition, QSAR analysis and docking studies. European Journal of Medicinal Chemistry 2015;105:156-170.

[18] Lv P, Cai T, Qian Y, Sun J, Zhu H. Synthesis, biological evaluation of chrysin derivatives as potential immunosuppressive agents. European Journal of Medicinal Chemistry 2011;46(1):393-398.

[19] Tran T, Vo T, Vo T, Cao T, Tran T. Synthesis and Evaluation of the Acetylcholinesterase Inhibitory Activities of Some Flavonoids Derived from Naringenin. The Scientific World Journal 2021;2021:1-10.

[20] Murti Y, Mishra P. Synthesis, Characterization, and Biological Evaluation of Novel Naringenin Derivatives as Anticancer Agents. Current Bioactive Compounds 2020;16(4):442-448.

[21] Duda-Madej A, Kozłowska J, Krzyżek P, Anioł M, Seniuk A, Jermakow K, Dworniczek E. Antimicrobial O-Alkyl Derivatives of Naringenin and Their Oximes Against Multidrug-Resistant Bacteria. Molecules 2020;25(16):3642.

[22] Kozłowska J, Potaniec B, Żarowska B, Anioł M. Synthesis and Biological Activity of Novel O-Alkyl Derivatives of Naringenin and Their Oximes. Molecules 2017;22(9):1485.

[23] Mingi C, Dong WK. Synthesis of 7-O-alkyl or 7-O-acyl Derivatives of Naringenin and Apigenin. Journal of the Korean Chemical Society 2020;64:2.

[24] Morris G, Goodsell D, Halliday R, Huey R, Hart W, Belew R, Olson A. Automated docking using a Lamarckian genetic algorithm and an empirical binding free energy function. Journal of Computational Chemistry 1998;19(14):1639-1662.

[25] Pettersen E, Goddard T, Huang C, Couch G, Greenblatt D, Meng E, Ferrin T. UCSF Chimera—A visualization system for exploratory research and analysis. Journal of Computational Chemistry 2004;25(13):1605-1612.

[26] BIOVIA, Dassault Systèmes; BIOVIA Discovery Studio Visualizer 2021. (accessed on 15 March 2023)

[27] Wang Y, Wang D, Dong B, Hao J, Jia X, Zhou H. Potential Candidate Molecule of Photosystem II Inhibitor Herbicide—Brassicanate A Sulfoxide. International Journal of Molecular Sciences 2024;25(4):2400.

[28] Zhang Q, Bai P, Zheng C, Cheng Y, Wang T, Lu X. Design, synthesis, insecticidal activity and molecular docking of doramectin derivatives. Bioorganic & Medicinal Chemistry 2019;27(12):2387-2396.

[29] Majhi P, Mansoori A, Pradhan U, Tripathi P, Shukla AK. Phytochemical Constituents in Essential Oil of Cymbopogon citrates and Exploring the Potential of Antifungal Activity for Management of Phytopathogenic Fungi. Journal of Plant Sciences and Crop Protection 2024;7.

[30] Enanoria M, Latorre M, Poliquit K, Fortugaliza S. In Vitro and In Silico Docking Techniques on Molluscicidal Activity of Tuba-Tuba (Jatropha curcas) and Santol (Sandoricum koetjape) Seed Against Golden Apple Snail (Pomacea Canaliculata L.) : A Potential Treatment for Preventing Crop Infestation in Rice Fields. International Journal of Research Publication and Reviews 2025;6(4):5496-5514.

[31] Sandhanam S, Ganesan P, Stalin A, Michael G, Balakrishna K, Pandikumar P, Ignacimuthu S, Naif A. Effect of compound isolated from Lawsonia inermis (L.) (Myrtales: Lythraceae) on the immature stages of filarial vector Culex quinquefasciatus Say (Diptera: Culicidae) and its docking analysis with Acetylcholinesterase (AChE1). Biocatalysis and Agricultural Biotechnology 2018;15:210-218.

[32] Daina A, Michielin O, Zoete V. SwissADME: a free web tool to evaluate pharmacokinetics, drug-likeness and medicinal chemistry friendliness of small molecules. Scientific Reports 2017;7(1):42717.

[33] Myung Y, de Sá A, Ascher D. Deep-PK: deep learning for small molecule pharmacokinetic and toxicity prediction. Nucleic Acids Research 2024;52(W1):W469-W475.

[34] Lee K, Lee IH, Kim HJ, Chang GS, Chung JE, No KT. The PreADME Approach: Web-based program for rapid prediction of physico-chemical, drug absorption and drug-like properties, EuroQSAR 2002 Designing Drugs and Crop Protectants: processes, problems and solutions. Blackwell Publishing, Massachusetts 2003;418-420.

[35] Pires D, Blundell T, Ascher D. pkCSM: Predicting Small-Molecule Pharmacokinetic and Toxicity Properties Using Graph-Based Signatures. Journal of Medicinal Chemistry 2015;58(9):4066-4072.

[36] Ecological Structure Activity Relationships (ECOSAR) Predictive Model.

[37] Abraham M, Murtola T, Schulz R, Páll S, Smith J, Hess B, Lindahl E. GROMACS: High performance molecular simulations through multi-level parallelism from laptops to supercomputers. SoftwareX 2015;1-2:19-25.